SOILS AND FOUNDATIONS Vol. 39, No. 4, 79–91, Aug. 1999
Japanese Geotechnical Society

FINGERING FLOW IN HOMOGENEOUS SANDY SOILS UNDER CONTINUOUS RAINFALL INFILTRATION

KEN KAWAMOTO[i] and TSUYOSHI MIYAZAKI[ii]

ABSTRACT

In order to establish a physical model leading to stable (uniform) and unstable (non-uniform fingering) flows in unsaturated soils, two-dimensional tests on continuous rainfall infiltration were carried out by changing not only the initial water content (air dry, 0.5%, 1.0%) but also the rainfall intensity (15, 30, 180 mm/h). The physical mechanism of fingering flow was discussed on the basis of precise suction measurements inside and outside the fingers.

The results show that wetting fronts developed in unsaturated sandy soils can be classified into three types; 1) fingering flow, 2) wavy front, and 3) plane front. Two types of fingering flow can be further distinguished by the difference of the swelling velocity; i.e., low-swell finger and high-swell finger flows. In each of the low-swell and high-swell fingers, a core and a swelling zone are developed while a finger is growing. Based on suction measurements inside them, it is found that the water condition in the finger core changes from wetting to drying processes while the water condition in the swelling zone remains in the wetting process. This hysteretic behavior in the core can be explained by the moisture distribution changing along a finger from tip to tail. Fingers swell when water moves from a finger core to surrounding dry sand. Such a swelling process is mainly controlled by the hydraulic conductivity for the wetting process at a finger tail.

Key words: fingering flow, hydraulic conductivity, infiltration, suction, unsaturated soil, wetting front (**IGC**: D4/E7)

INTRODUCTION

When raindrops infiltrate into unsaturated soil, a wetting front is generated and moves downward until reaching the groundwater level. A problem arises from the fact that the wetting front never moves uniformly, but rather heterogeneously with growing finger-like flow. It is well known that such a heterogeneous flow, called the fingering flow, is developed as a result of instability at the wetting front. If fingering flow starts, preferential pathways are formed in unsaturated soils, and water-borne contaminants are rapidly transported downward through these pathways until reaching groundwater (Kung, 1990; Hillel, 1993). It can be easily understood, accordingly, that the fingering flow must be a key factor to solve the following engineering problems; 1) how to evaluate, safely, the environmental damage arising from disposing of industrial wastes in soils, 2) how to recharge effectively the groundwater in arid and semi-arid regions and water-repellent sandy soils (e.g., de Rooij, 1995), and 3) how to accelerate desalinization for improving saline soils (Kawamoto et al., 1996). Heavy metal ions and even radio active nuclides, for example, can migrate through the fingering flow so rapidly that the environment is damaged widely, as well as quickly. In order to prevent such damage, on some scientific bases, soil engineers must understand at least the reality of the fingering flow through unsaturated soils. It is of particular importance to realize that the fingering flow greatly accelerates the migration of these dangerous materials.

Steenhuis et al. (1996) recognized two types of fingering flows; heterogeneity-driven finger and gravity (instability)-driven finger. In the field, some fingering flows are driven by heterogeneity (or discontinuity) in soil structure where macro-pores or cracks exist. Fingering flow, however, does occur in homogeneous soils. The occurrence and the types of fingering flow, even if homogeneous soils are concerned, are sensitively affected by many factors such as initial water content, sizes and distribution of soil particles, infiltration rate, and so on (Tamai et al., 1987; Baker and Hillel, 1990; Selker et al., 1992 (a); Cho, 1995; Yao and Hendrickx, 1996). A slight increase of the initial water content, for example, damps down the occurrence of fingering flow (Diment and Watson, 1982; Annaka and Idesawa, 1996).

An important characteristic of fingering flow is that once fingering flow appears, water flows continuously through these pathways without changing their locations and shapes. Tabuchi (1961) has suggested that the suction distribution inside a growing finger may play a cru-

[i] Assistant Professor, Faculty of Engineering, Saitama University, Urawa 338-8570.
[ii] Associate Professor, Graduate School of Agricultural and Life Sciences, The University of Tokyo.
Manuscript was received for review on November 21, 1997.
Written discussions on this paper should be submitted before March 1, 2000 to the Japanese Geotechnical Society, Sugayama Bldg. 4F, Kanda Awaji-cho 2-23, Chiyoda-ku, Tokyo 101-0063, Japan. Upon request the closing date may be extended one month.

cial role in deciding its shape and size. Liu et al. (1991) measured suction change in a growing finger, and found that the suction increases just after a finger tip passes. They stated, based on the test results, that the suction increase is probably due to the fact that water condition in a growing finger is switched from wetting to drying process. They also found that lateral flow of water, from a finger core to the surrounding dry zone, ceases when the suction at a finger core exceeds the water entry suction defined by a wetting curve on the corresponding water characteristic curve.

It is important to point out, however, that finger flow only maintains its shape and size for a relatively short period of time. If the flow continues for a long period of time, lateral water movement leads to significant swelling of the finger. In tests by Glass et al. (1989) and Glass and Nicholl (1996), for example, water flow was continued for tens or hundred of hours to produce such a swelling finger. They suggest that the lateral water movement takes place by means of film flow and vapor diffusion. Kawamoto et al. (1996) also observed the swelling fingers in a short, as well as a long, period test under continuous rainfall, and distinguished two types of fingering flow; i.e., low-swell finger and high-swell finger.

In order to understand further what controls the separation between stable (uniform) and unstable (non-uniform fingering) flows in unsaturated soils, we carried out two-dimensional flow tests under continuous rainfall infiltration. The final objectives are: first to clarify the physical mechanism leading to these various types of finger (non-uniform) flows on the basis of precise suction measurements; and second, to build up, for practical use, a more realistic model which makes it possible to simulate non-uniform flow through unsaturated soils, rather than the conventional approach based on homogeneous flow. In this paper, however, we will mainly deal with the first target.

EXPERIMENT

Material and Method

Figure 1 shows an experimental apparatus composed of an acrylic board container with inside dimensions of 50 cm wide, 50 cm high and 1 cm thick, a rainfall simulator, and drain pipes. The thickness, 1 cm, was selected such that two-dimensional flow is generated. Ten boxes 50 cm wide and 5 cm high were stacked, after being filled sand, one by one to assemble the container.

Toyoura sand, a fine uniform sand, was used in the present study. 99.7% in weight is retained between 0.21 mm and 0.105 mm sieves. The sand was washed by mixing it in a dilute solution of soap, rinsed out ten times with distilled water, and then air-dried. Three different initial water contents were prepared; i.e., air-dry (0.0%), 0.5%, and 1.0% (Table 1). To get these water contents, the air-dried sand was thoroughly mixed with a proper amount of distilled water in a plastic bag, stored in a dark room for more than 24 hours, and then packed in the container before a test. To keep the sand as uniform

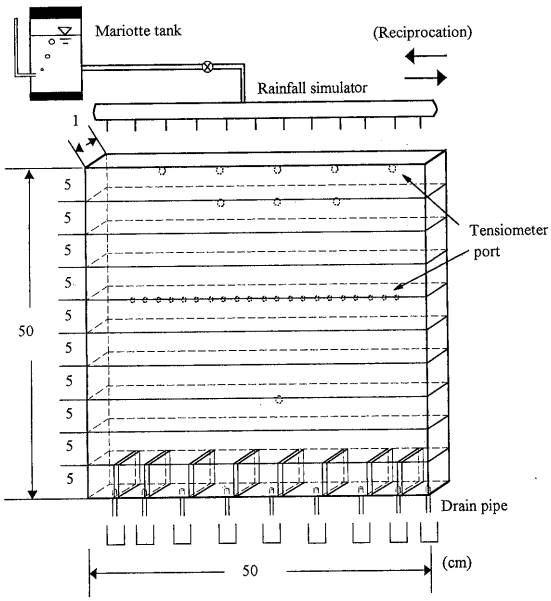

Fig. 1. Experimental apparatus

Table 1. Experimental conditions

Initial water content (w_i)	Rainfall intensity (I_R)		
	15 mm/h	30 mm/h	180 mm/h
Air dry (0.0%)	Run 1	Run 2	Run 3
0.5%	Run 4	Run 5	Run 6
1.0%	Run 7	Run 8	Run 9

as possible, the bottom box of the container was first filled with the sand by hand. Then a new box was stacked on it, and was filled with the sand again. The dry bulk density was 1.58 g/cm^3 in all tests. The coefficient of hydraulic conductivity, under a saturated condition, was also measured at 781 mm/h at 20°C by a constant head permeability test.

Suction change was measured during the tests by means of transducerized tensiometers installed at ports on the back wall of the container at four different depths from the top surface (Fig. 1); i.e., 5 ports at 2.5 cm depth, 3 ports at 7.5 cm depth, 40 ports at 22.5 cm depth, and 1 port at 37.5 depth, respectively. A tensiometer was fasten at each port so as to be flush with the inside surface of the container. Two different sizes of porous cups were made from a fritted glass plate of 0.5-5 μm thick; i.e., 10 mm in diameter and 2 mm thick for the ports at three depths of 2.5, 7.5, 37.5 cm; and 6 mm in diameter and 1 mm thick for the ports at 22.5 cm depth. The bottom box of the container was divided into 9 parts, each of which was connected to a drain pipe.

Rainfall was simulated by a rainfall simulator which consisted of a rainfall acrylic pipe with 12 needles and a mariotte tank (Fig. 1). A uniform flux was given by dropping water at a constant rate from the needles using DC motor (a reciprocation of 1.2 sec cycle and 2 cm amplitude). Three rainfall intensities (I_R mm/h) were used;

i.e., 15, 30, and 180 mm/h (Table 1). The rainfall intensity of 15 mm/h was a lower limit to get a uniform rainfall flux in the present rainfall simulator. In all tests, water drained from each drain pipe was collected at a constant interval. Water was applied until cumulative drainage of 2,000 cm^3 (40 cm) had been obtained. Wetting fronts during the course of experiments were recorded on videotape using a video camera and on still film using a still camera.

Nine tests were done by changing initial water content w_i and rainfall intensity I_R. For simplicity, each test will be identified by the number of test run as shown in Table 1. For example, Run 4 means a test done with $w_i=0.5\%$ and $I_R=15$ mm/h.

TEST RESULTS AND DISCUSSION

Types of Wetting Fronts and Their Classification

All wetting fronts observed in the nine tests are traced in Fig. 2. One important observation is that these wetting fronts can be classified, according to their shapes, into three types; 1) fingering flow, 2) wavy front, and 3) plane

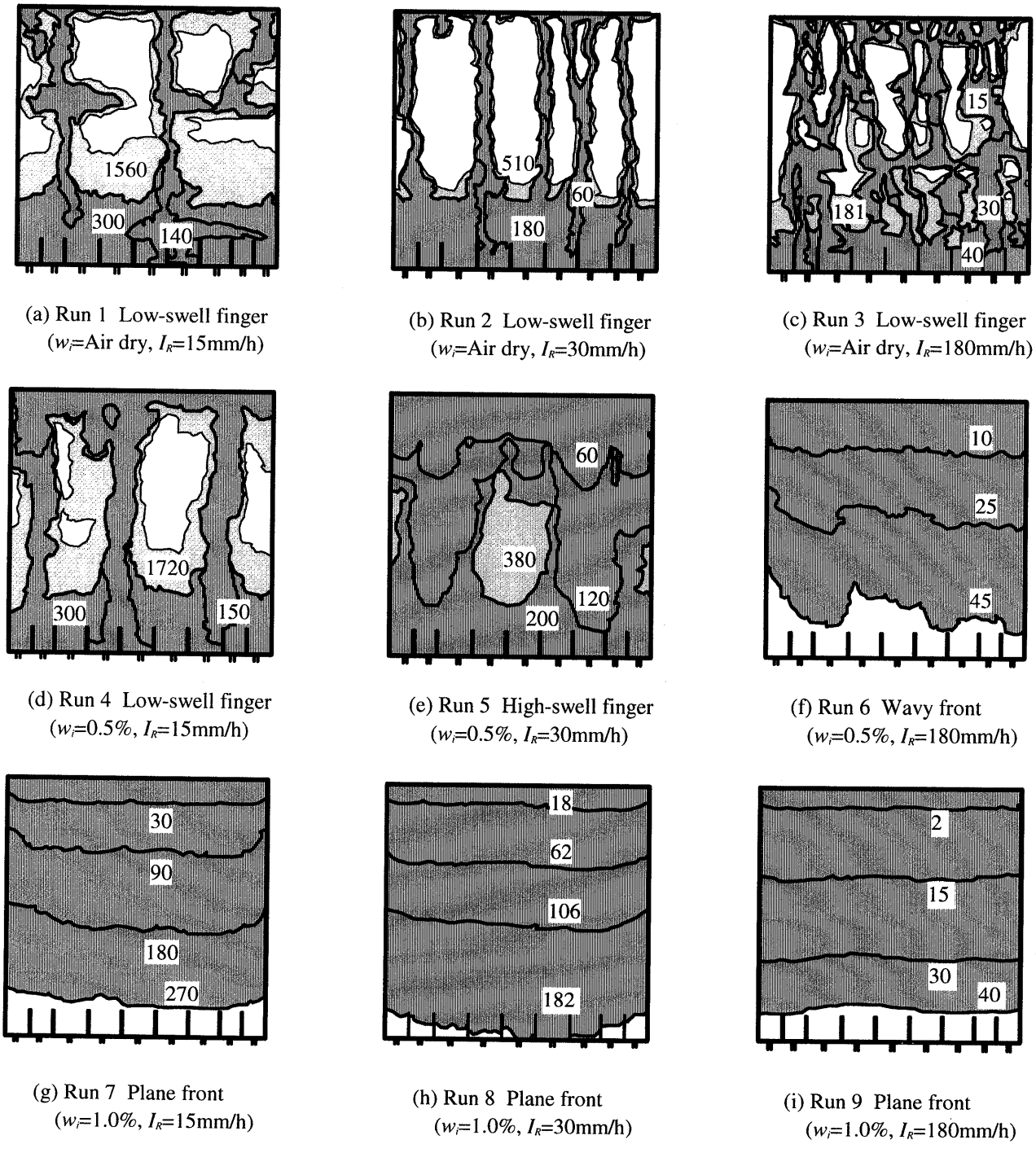

(a) Run 1 Low-swell finger (w_i=Air dry, I_R=15mm/h)

(b) Run 2 Low-swell finger (w_i=Air dry, I_R=30mm/h)

(c) Run 3 Low-swell finger (w_i=Air dry, I_R=180mm/h)

(d) Run 4 Low-swell finger (w_i=0.5%, I_R=15mm/h)

(e) Run 5 High-swell finger (w_i=0.5%, I_R=30mm/h)

(f) Run 6 Wavy front (w_i=0.5%, I_R=180mm/h)

(g) Run 7 Plane front (w_i=1.0%, I_R=15mm/h)

(h) Run 8 Plane front (w_i=1.0%, I_R=30mm/h)

(i) Run 9 Plane front (w_i=1.0%, I_R=180mm/h)

Fig. 2. Tracings of wetting fronts (The numbers in diagrams refer to the time after rainfall (min))

front. The fingering flow developed, in particular, in Runs 1 to 5 in which all tests were done at the initial water contents of air dry (0.0%) and w_i=0.5%. The plane wetting fronts, on the other hand, developed in Runs 7 to 9 tested under the initial water content of w_i=1.0%. The plane front had a stable wetting front without disturbing the shape under continuous water supply from the surface (Fig. 2(g), (h), (i)). In Run 6, the wavy front looks intermediate between the fingering flow and the plane front. This wavy front developed its wave with depth but never grew into a fingering flow (Fig. 2(f)).

It seems important to note, in Fig. 2, that the fingering flow expanded only slightly in the cases of Runs 1 to 4, but expanded remarkably in Run 5. This implies that fingering flow can be further classified into 1) low-swell finger and 2) high-swell finger, as has already been pointed out by Kawamoto et al. (1996). Here the low-swell finger is defined, on a tentative basis, as a type of fingering flow which maintains its flow pattern, without swelling much, during a short period of time (say, a few hours) under continuous water infiltration. The high-swell finger is defined as a type of fingering flow which expands its width for a short period. The former type has been observed in many laboratory tests (e.g., Glass et al., 1989). The differences of the two types of fingering flow will be discussed later in terms of the swelling velocity.

Based on these observations, it can be said that the initial water content, rather than the rainfall intensity, is a dominant factor controlling the types of wetting fronts. Under the air-dry condition (Fig. 2(a), (b) and (c)), the low-swelling finger is generated irrespective of the rainfall intensity ranging from 15 to 180 mm/h. With an initial water content of 1.0% (Fig. 2(g), (h) and (i)), on the other hand, the plane front is generated irrespective of the rainfall intensity from 15 to 180 mm/h. With an intermediate water content of 0.5%, the wetting front changes, with the increasing rainfall intensity, from the low-swell finger (Fig. 2(d)) to the wavy front (Fig. 2(f)) via the high-swell finger (Fig. 2(e)). The types of wetting fronts in each test are summarized in Table 2.

Diment and Watson (1982) reported such a change of wetting front from the unstable (fingering) front to the stable (plane) one by increasing the initial water content. Yao and Hendrickx (1996) also observed the change in wetting fronts which were generated in air dry homogeneous sand layers under various rainfall intensities. They found that the wetting front was unstable (fingering) at a rainfall intensity between 3 and 120 mm/h, semi-stable (wavy) at a rainfall intensity between 1.2 and 3 mm/h, and stable (plane) at a rainfall intensity lower than 1.2 mm/h. Their result is in accordance with our result showing that fingering flow occurs under the air dry condition. At the initial water content of 0.5%, however, the wetting front changes from unstable to semi-stable with increasing rainfall intensity (Fig. 2(d), (e) and (f)). This suggests that the trend from unstable to stable with increasing rainfall intensity could be reversed depending on the initial water content.

It can be said, in general, that wetting fronts in homogeneous sandy soils become more and more stable with increasing initial water content when rainfall intensity is kept constant. It is very difficult to say, however, what kind of wetting front is developed in initially dry sands because not only the slight increase of initial water content but also the change of rainfall intensity have such a significant effect on the type of fingers actually developed. Furthermore, the types of wetting fronts vary due to many factors such as size and distribution of soil particles, precleaning of sands, and so on (Baker and Hillel, 1990; Yao and Hendrickx, 1996; Glass et al., 1989). All of this makes it difficult to accurately predict which type of wetting front will occur in initially dry sands correctly, and to give the exact information about the reoccurrence of types of wetting fronts under the same experimental conditions.

Table 2. Types of wetting fronts

Initial water content (w_i)	Rainfall intensity (I_R)		
	15 mm/h	30 mm/h	180 mm/h
Air dry (0.0%)	Low-swell finger (Run 1)	Low-swell finger (Run 2)	Low-swell finger (Run 3)
0.5%	Low-swell finger (Run 4)	High-swell finger (Run 5)	Wavy front (Run 6)
1.0%	Plane front (Run 7)	Plane front (Run 8)	Plane front (Run 9)

Table 3. Numbers, maximum and minimum growing velocity of fingers

Experiment	Numbers	Max. growing velocity (cm/min)	Min. growing velocity (cm/min)
Run 1 (w_i=Air dry, I_R=15 mm/h)	4	0.52	0.07
Run 2 (w_i=Air dry, I_R=30 mm/h)	6	1.13	0.33
Run 3 (w_i=Air dry, I_R=180 mm/h)	15	1.80	1.33
Run 4 (w_i=0.5%, I_R=15 mm/h)	4	0.40	0.01
Run 5 (w_i=0.5%, I_R=30 mm/h)	3	0.46	0.06

Morphological Properties of Fingering Flow

A horizontal wet layer was first formed just below the ground surface. After that, fingering flow started to develop (Fig. 2(a) to Fig. 2(e)). The wet layer was called the distribution layer (Ritsema and Dekker, 1995) or the induction zone (Hill and Parlange, 1972; Selker et al., 1992 (b)), and was believed to play a role in distributing supplied water from the upper wet zone to each finger. The thickness values of the distribution layers, just after fingering flows started, were about 1 cm in Runs 1 to 3 (w_i=air dry), 2 cm in Run 4 (w_i=0.5%), and 5 cm in Run 5 (w_i=0.5%).

The number of fingers generated in each test and their maximum and minimum growing velocities are summarized in Table 3. The growing velocity of a finger was calculated from the passage time between 20 cm and 40 cm below the top surface. Each finger grows at a rather constant rate, but the growing velocity changes markedly

from finger to finger; the more the rainfall intensity increases, the more the number of low-swelling fingers increases and the growing velocity becomes faster.

A few fingers were sometimes merged to make a single finger, which occurred in parallel with their swelling during downward movement. This happened in low-swell and high-swell fingers, but especially in Run 3 (as shown in Fig. 2(c)), since many fingers were generated in parallel. Since the swelling and merging of fingers took place simultaneously in Run 5, the whole observed zone looked wetted uniformly at 380 min after the test started.

In Runs 1 to 5 (Fig. 2(a) to Fig. 2(e)), horizontal wet zones were formed at the bottom of the containers after fingers reached the drain pipes open to the atmosphere. These zones spread at about 10 cm height at the start of drainage from the drain pipes. Furthermore, they spread slowly upward for the duration of rainfall and reached a maximum height of 20 cm in Run 1. It is difficult to determine the influence of these wet zones on the fingering flows, so in this paper the authors have separated these zones from fingering flows.

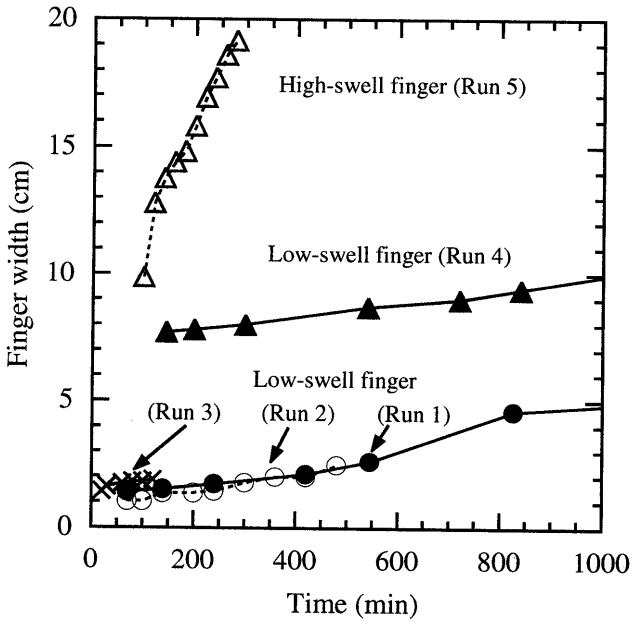

Fig. 3. Increase in finger width with elapsed time

During downward movement of a finger, it was found that the finger consisted of two areas; i.e., an inner core and a surrounding outer area (Hill and Parlange, 1972; Glass et al., 1989). Glass et al. (1989) visualized fingers by transmission of light and observed the formation of these areas. The inner core was formed simultaneously with the pass of the wetting front, and conducted most of the flow. The surrounding outer area (called the "fringe area" by Glass et al. (1989)) was formed by the lateral water movement from the core (this means that the finger width swells). The formation of the surrounding outer area was, in general, slow, having a time scale in the order of days. In this paper, we call the inner core the "core zone" and the surrounding outer area the "swelling zone."

In Fig. 3, widths of five fingers are shown as a function of elapsed time. The width was measured at 22.5 cm depth, only when the finger was isolated and was moving downward without merging with neighboring fingers. It can be seen, from Fig. 3, that the width in both low-swell and high-swell fingers increases linearly with elapsed time. In Table 4, the finger widths measured at an early stage of growth (core zone) and at a final stage (core zone+swelling zone) are tabulated together with the swelling velocities, which were calculated from the gradients of linear regression curves for the plots in Fig. 3. The swelling velocities of the low-swell fingers are within 0.12 to 0.26 cm/h, while the swelling velocity of the high-swell finger is 2.77 cm/h, about ten times faster than those of the low-swell fingers. These results give a criterion for making a distinction between two types of fingering flow in this experiments; i.e., low-swell fingers whose swelling velocity is far less than 1 cm/h, and high-swell fingers whose swelling velocity is larger than 1 cm/h. During the early stage, all widths of the low-swell fingers fall within 1.0 to 1.4 cm in the case of the air-dry sand. In the case of the moist sand (w_i=0.5%), however, the widths are wider (7.7 and 9.9 cm), which indicates that the width depends much on the initial water content.

Suction Changes in Finger Core Zones

Suction changes were measured at several tensiometer

Table 4. Finger width at early stage of growth and at rainfall halt, swelling velocity of fingers

Experiment	Finger width (cm)		Swelling velocity of finger (cm/h)	Correlation coefficient
	At early stage of growth	At final stage when rainfall halt		
Run 1 Low-swell finger (w_i=Air dry, I_R=15 mm/h)	1.4 (t=70 min)	7.9 (t=1925 min)	0.21	0.99
Run 2 Low-swell finger (w_i=Air dry, I_R=30 mm/h)	1.0 (t=70 min)	2.5 (t=480 min)	0.21	0.98
Run 3 Low-swell finger (w_i=Air dry, I_R=180 mm/h)	1.4 (t=20 min)	1.9 (t=120 min)	0.26	0.94
Run 4 Low-swell finger (w_i=0.5%, I_R=15 min/h)	7.7 (t=145 min)	10.9 (t=1860 min)	0.12	0.98
Run 5 High-swell finger (w_i=0.5%, I_R=30 mm/h)	9.9 (t=100 min)	19.2 (t=280 min)	2.77	0.98

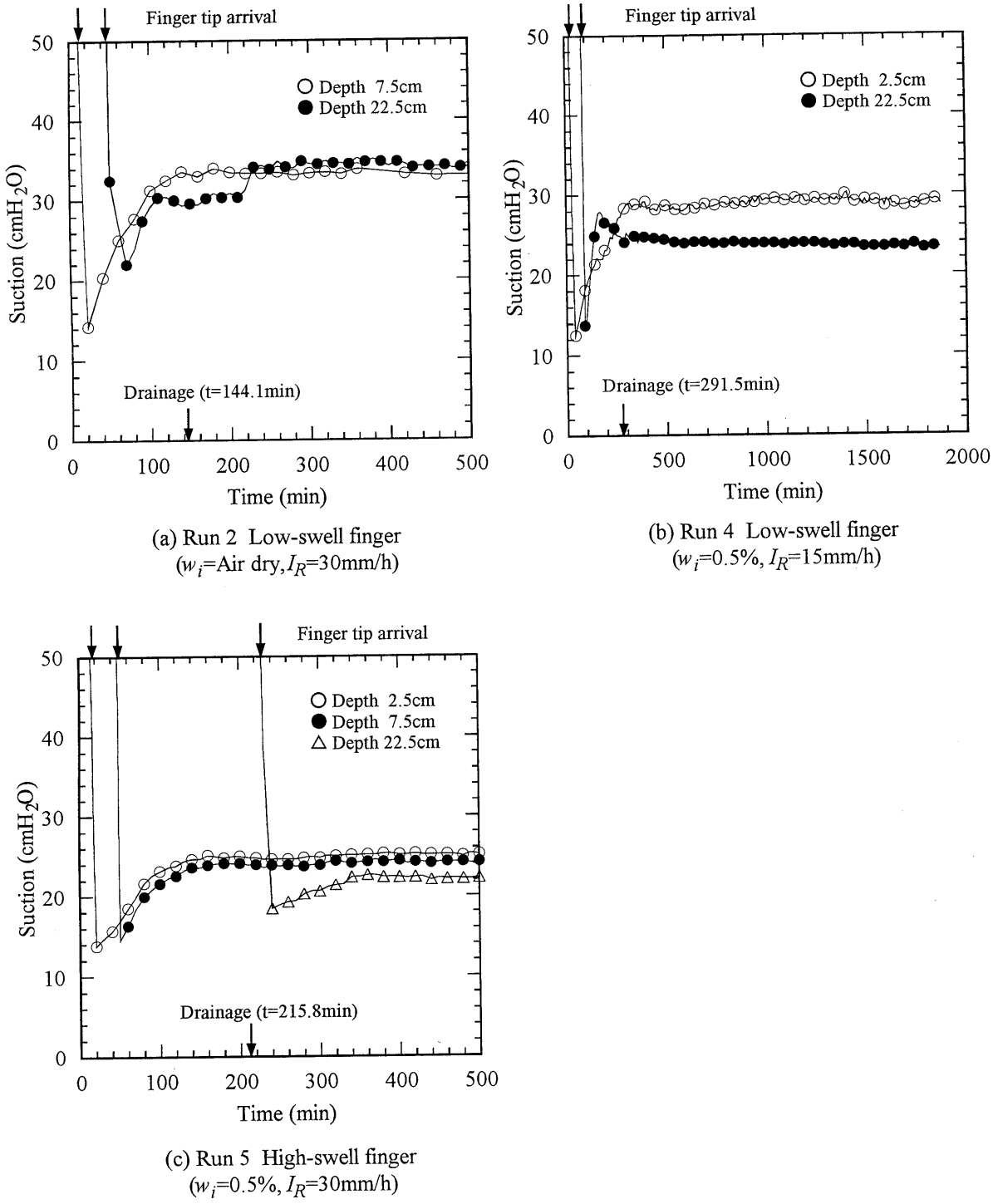

(a) Run 2 Low-swell finger (w_i=Air dry, I_R=30mm/h)

(b) Run 4 Low-swell finger (w_i=0.5%, I_R=15mm/h)

(c) Run 5 High-swell finger (w_i=0.5%, I_R=30mm/h)

Fig. 4. Suction changes in finger core zones at each depth

Table 5. Bottom values of suction at each depth

Depth (cm)	Bottom values of suction (cmH_2O)		
	Run 2 Low-swell finger (w_i=Air dry, I_R=30 mm/h)	Run 4 Low-swell finger (w_i=0.5%, I_R=15 mm/h)	Run 5 High-swell finger (w_i=0.5%, I_R=30 mm/h)
2.5	—	11.9 (t=35 min)	13.3 (t=18 min)
7.5	14.3 (t=20 min)	—	14.6 (t=49 min)
22.5	22.0 (t=70 min)	13.0 (t=91 min)	18.4 (t=240 min)

ports through which fingers were passing (finger core zones). The results are shown in Fig. 4 as a function of elapsed time. In all three figures, the arrow on the bottom line indicates the time when the drainage started from drain pipes, and the depth indicates where each tensiometer ports was installed. The following observations are worth noticing.

Very high suctions are recorded until finger tips arrive at the positions where the tensiometers were installed. The suctions suddenly drop to bottom values when the finger tips arrive (stage 1), and are followed by slight recovery up to steady values (stage 2). After that, the suction remains almost constant at the steady value (stage 3). Here, the bottom value refers to the smallest value of suction recorded at each tensiometer port. (It should be noted, however, that there exist some deviations from the general trend; e.g., the suction measured at 22.5 cm depth in Run 2 increases again up to another steady value at 240 min in stage 3 (Fig. 4(a)); in Fig. 4(b), the suction measured at 22.5 cm depth in Run 4 decreases slightly between 180 min and 320 min in stage 2.) In Table 5, the bottom values of suction measured at the end of stage 1 are tabulated at each depth. It should be noted that the bottom value is higher when the finger tip moves deeper.

In order to calculate vertical suction gradients in the low-swell and high-swell fingers, the suction difference, as well as the distance, between two tensiometer ports were determined at stages 2 and 3 by using the data in Fig. 4. In doing this, the vertical axis was taken positive downward. This means that the negative suction gradient acts so as to suppress the downward flow in fingers, while the positive suction gradient accelerates the downward flow. As summarized in Table 6, these suction gradients change from negative to positive in Run 2 and from positive to negative in Run 4. More importantly, the vertical suction gradients are very small, almost zero, in both of the low-swell and high-swell fingers during stage 3. So it can be concluded that downward flow of water along a core of each finger is mainly conducted by the gravitation-

Table 6. Vertical suction gradients in low-swell and high-swell fingers

(a) Run 2 Low-swell finger (w_i=Air dry, I_R=30 mm/h)

Depth (cm)	Stage 2 (t=80 min)		Stage 3 (t=500 min)	
	Suction (cmH_2O)	Suction gradient	Suction (cmH_2O)	Suction gradient
7.5	27.8	−0.25	33.1	0.10
22.5	24.0		34.6	

(b) Run 4 Low-swell finger (w_i=0.5%, I_R=15 mm/h)

Depth (cm)	Stage 2 (t=200 min)		Stage 3 (t=1800 min)	
	Suction (cmH_2O)	Suction gradient	Suction (cmH_2O)	Suction gradient
2.5	23.2	0.18	29.2	−0.28
22.5	26.8		23.7	

(c) Run 5 High-swell finger (w_i=0.5%, I_R=30 mm/h)

Depth (cm)	Stage 2 (t=220 min)		Stage 3 (t=500 min)	
	Suction (cmH_2O)	Suction gradient	Suction (cmH_2O)	Suction gradient
2.5	23.9	−0.26	25.2	−0.18
7.5	22.6	—	24.3	−0.13
22.5	—		22.3	

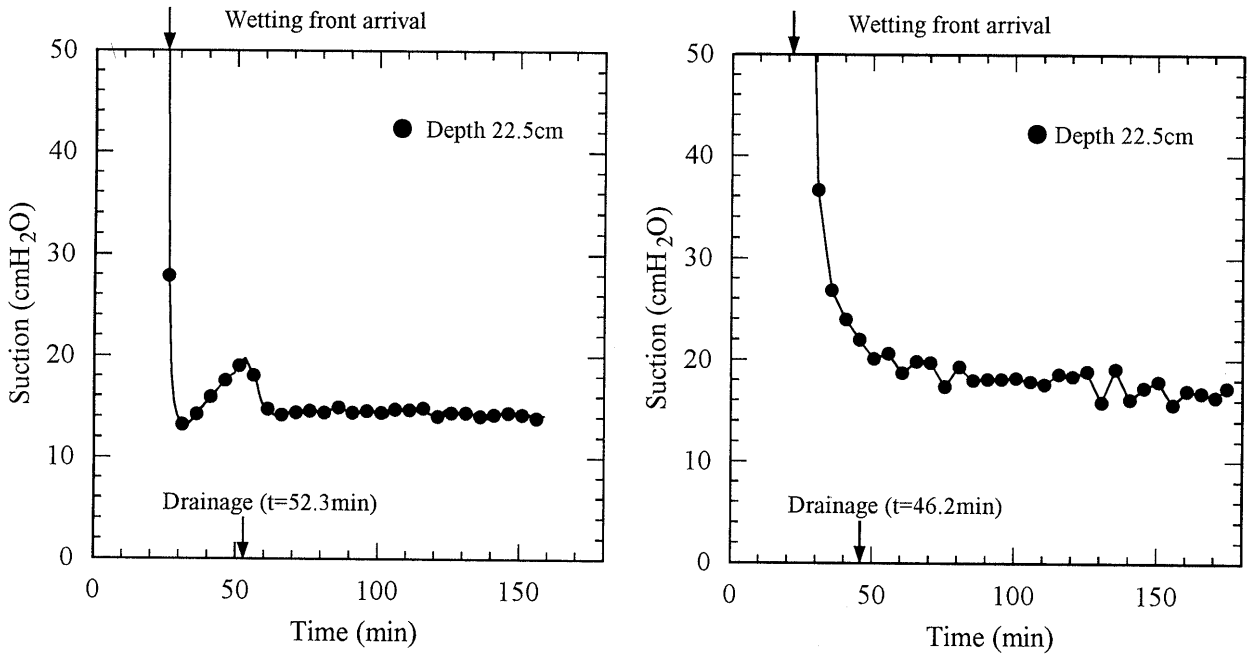

(a) Run 6 Wavy front (w_i=0.5%, I_R=180mm/h)

(b) Run 9 Plane front (w_i=1.0%, I_R=180mm/h)

Fig. 5. Suction changes of wavy and plane fronts

al gradient.

The suction changes for the wavy-front in Run 6 and the plane front in Run 9 are shown in Fig. 5, with the following observations. In the case of the wavy front (Fig. 5(a)), the suction first drops sharply to a bottom value when the wetting front arrives, and then increases a little. When drainage starts from the bottom, the suction decreases again and finally reaches a steady value. In the case of the plane front (Fig. 5(b)), the suction also decreases sharply when the wetting front arrives, but continues to decrease gradually with time.

All data clearly show that the suction increases when either a finger tip or a wetting front has passed. This occurs in the three types of unstable flow (i.e., low-swell finger, high-swell finger, and wavy front), which means clearly that a suction gradient behind a finger tip or a wetting front tends to suppress the downward flow. This finding is in accordance with earlier observations (Baker and Hillel, 1990; Selker et al., 1992 (b)), and analytical stability criteria (Raats, 1973; Philip, 1975).

Moisture Profile from Finger Tip to Tail

In Figs. 4, the three successive stages (1 to 3) were distinguished based on the suction change at each tensiometer port. Such a suction change is caused by the moisture profile inside a finger. Glass et al. (1989) found that a growing finger consists of three zones at least; 1) a finger tip with the highest water content, 2) a transferring zone behind the finger tip, and 3) a finger tail with a constant water content. From this point of view, it is quite natural to observe that stages 1 to 3 appear in sequence when a finger, with these three regions, is passing through a tensiometer port. It can also be pointed out that the water content at a finger tip is lost during downward movement since the suction at the tip gradually increases with the depth of the tensiometer port (Table 5).

Water characteristic curves for Toyoura sand were determined by the so-called soil column method. The dry bulk densities of the soil columns were equal to the two-dimensional tests (1.58 g/cm^3). The results are summarized in Fig 6. The main drying curve was obtained from drying the sand initially saturated, and the wetting curves by wetting the sands with the initial water contents of air dry (0.0%) and 0.5%. Water content at a given suction in the wetting curves is smaller than in the main drying curve because of the entrapped air. Note that the method by van Genuchten (1980) yields the solid curves in the figure to fit the water content-suction data experimentally determined. Note also that the two dotted lines in the same figure are hysteretic curves which will be obtained when the wetting curves are dried again. Using these water content-suction curves, we can discuss, in detail, the suction change (Fig. 4) and the corresponding moisture profile inside a finger.

The suction change in Run 2 (Fig. 4(a)) can be interpreted using the paths ① and ② in Fig. 6 which are the water content-suction curves for the wetting and drying processes initiated from an air dry condition, as follows. The sudden decrease of suction in stage 1 corresponds to a step-wise increase of water content in the wetting path ①, and the suction recovery in stage 2 is given by the drying path ②. The almost constant suction in stage 3 means that the suction and water content both remain at a point denoted by the open arrow on ②. Similarly, in the cases of Run 4 and Run 5 (Fig. 4(b) and (c)), stage 1 is on ③ which is the water content-suction curve for the wetting process started from the water content of 0.5%, and stage 2 is on ④ for the corresponding drying process. An important point is, therefore, that the suction change in Fig. 4 arises from switching the water condition from wetting to drying when a finger tip, irrespective of the type of fingering flow, is passing. Note also that the hys-

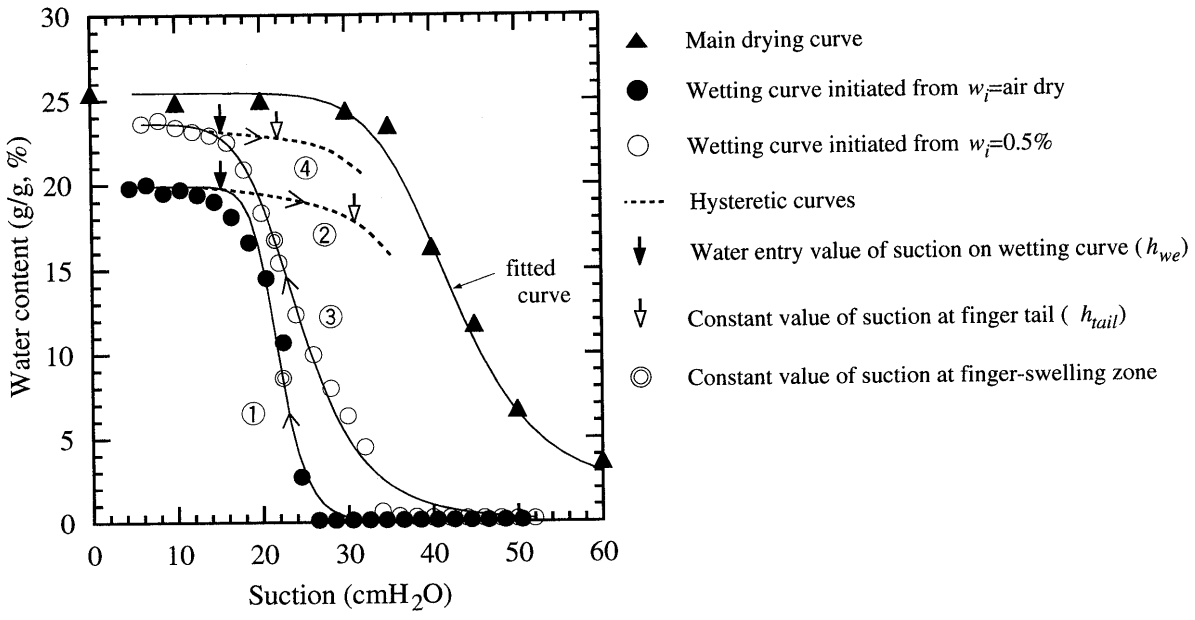

Fig. 6. Water characteristic curves

teretic behavior from wetting to drying is caused by the moisture profile composed of the three successive zones (Glass et al., 1989).

By analyzing wetting tests initiated from the initial water contents of air dry and 0.5%, the water entry suction (the limit of capillary rise of water) for the Toyoura sand can be determined at about 16 cmH_2O (Miyazaki, 1993; Bouwer, 1966). It is interesting to note that the water condition in a growing finger changes from wetting to drying at a value close to the water entry suction (Table 5). This may be explained by the fact that the water does not infiltrate into the dry sand before the suction in the finger tip reaches the water entry value, as also discussed by Hillel and Baker (1988) and Liu et al. (1991). When the wetting front first arrives at the dry sand, the infiltrating water is under too high a suction to allow its entry into the pores of the dry sand. The distribution layer formed below the ground surface also continues to deliver water toward the finger tip. Hence, the suction in the finger tip falls to a value permitting entry of water, and this value may be predictable from the wetting tests (the limit of capillary rise of water in the dry sands).

Hydraulic conductivities of the Toyoura sand are reported in Fig. 7 as a function of suction. The conductivity in the main drying process initiated from full saturation (dry bulk density of 1.58 g/cm^3) was determined from a steady-state method with a suction plate (Shiozawa, 1983). The hydraulic conductivities in the wetting process initiated from the initial water contents of air dry and 0.5% were estimated by means of optimized parameters of the water characteristic curves in Fig. 6 (van Genuchten, 1980), and are shown by the two broken lines in Fig. 7. It is important to note that the estimated hydraulic conductivities in the wetting process decrease drastically when the suction is bigger than the water entry suction denoted by the solid arrow. This effect appears clearly in the case of the wetting process initiated from the air dry.

Comparing the water entry suction (h_{we}) with the constant suction at a finger tail (h_{tail}), we can discuss whether water can move laterally from the central core of a finger to surrounding dry sand. In the case of the low-swell finger in Run 2 (Fig. 4(a)), the values of h_{tail} are 33 and 34 cmH_2O in suction at 7.5 and 22.5 cm depth, respectively, and exceed the value of h_{we}. In this case, the hydraulic conductivity is very small, within a range from 10^{-8} to 10^{-10} cm/s. These facts suggest that very small, if any, lateral water movement takes place from the central core of a finger into the surrounding dry sand. In the case of the high-swell finger in Run 5 (Fig. 4(c)), on the other hand, the values of h_{tail} are about 25, 24 and 22 cmH_2O in suction at 2.5, 7.5 and 22.5 cm depth, respectively. Note that these values are very close to h_{we}, and that the hydraulic conductivity, 10^{-3} to 10^{-4} cm/s, is substantially high. These facts strongly suggest that water moves laterally to swell the finger.

Suction Changes in Finger-Swelling Zones

To measure suctions in finger-swelling zones, tensiometer ports were arranged laterally at 22.5 cm depth (Fig. 1). For convenience, a horizontal axis x was chosen such that the left edge of the container was $x=0$ cm (Fig. 9). The exact positions of tensiometers and the successive swelling of fingers are sketched in Fig. 9. The suction changes at $x=29$ cm (Fig. 8(a)) and at $x=24$, 26 cm (Fig. 8(b)) were measured at 800 min, 1200 min, and 1700 min after the start of rainfall, respectively.

Suction change in a finger-swelling zone consists of two stages as shown in Fig. 8. The first stage is the initial portion ending in a sudden decrease in suction which

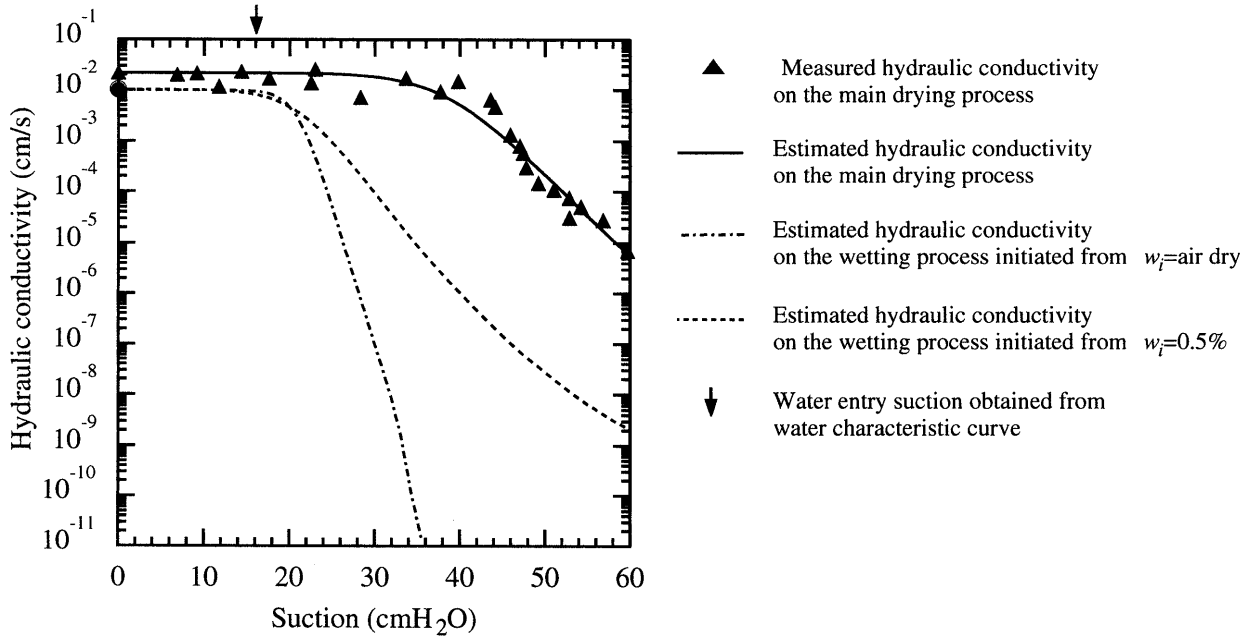

Fig. 7. Hydraulic conductivity-suction curves

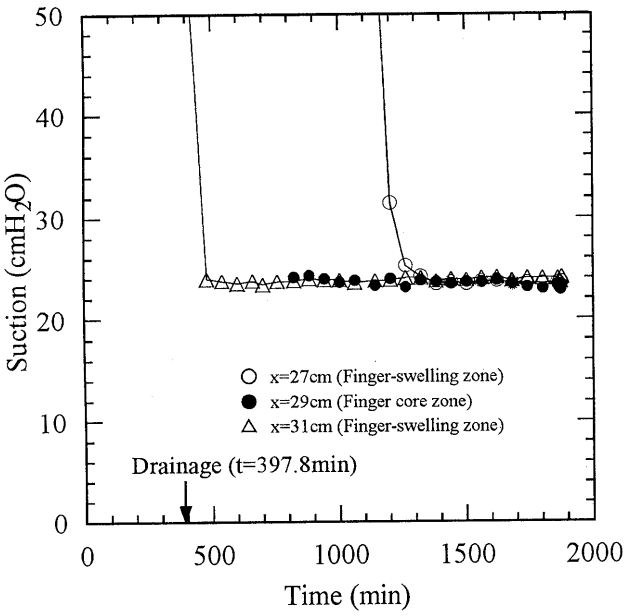

(a) Run 1 Low-swell finger
(w_i=Air dry, I_R=15mm/h)

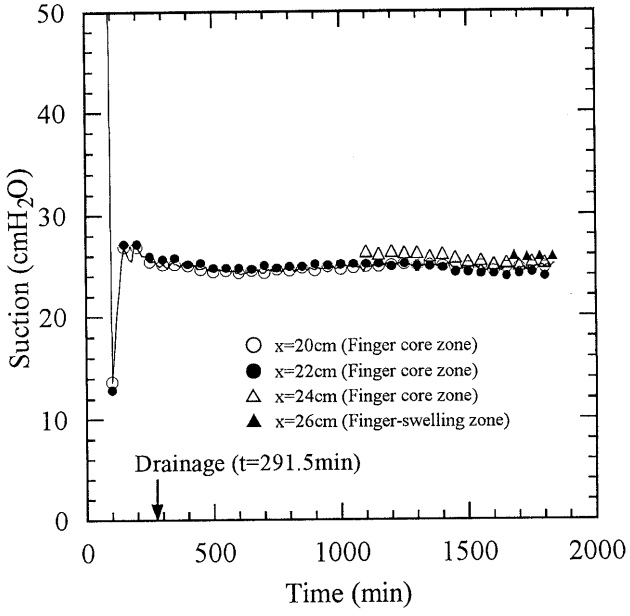

(b) Run 4 Low-swell finger
(w_i=0.5%, I_R=15mm/h)

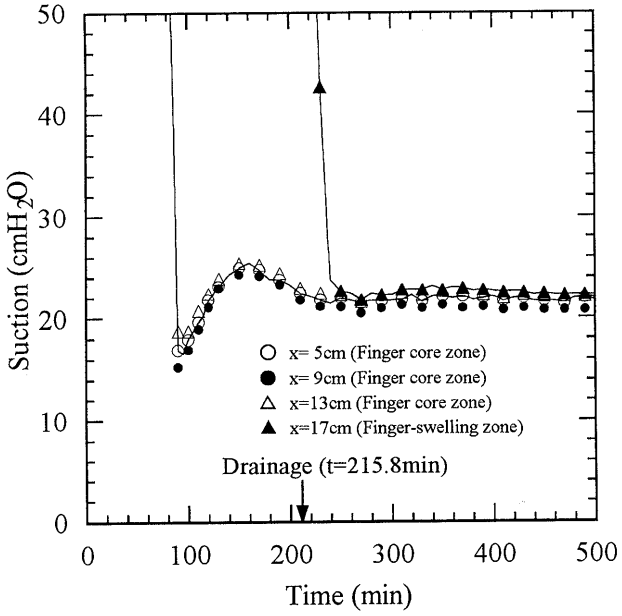

(c) Run 5 High-swell finger
(w_i=0.5%, I_R=30mm/h)

Fig. 8. Suction changes in finger-swelling zones with neighboring finger core zones

takes place when a swelling zone passes through the tensiometer port; and the second stage is the steady state keeping suction almost constant.

In order to calculate horizontal suction gradients in the low-swell and high-swell fingers, the suction difference, as well as the horizontal distance, between two tensiometer ports was measured twice during a test. The results are summarized in Table 7. The horizontal suction gradient, in fact, exists at the center of the low-swell finger at x=29 cm (a finger core) in both outward directions (finger swelling zones) (Table 7(a) and Fig. 9(a)). Inside finger core zones, the horizontal suction gradient also exists at the center of the finger in directions toward the outside (Table 7(b), 7(c) and Fig. 9(b), 9(c)).

In the case of the high-swell finger in Run 5, the horizontal suction gradient is 0.03 at =280 min, and is

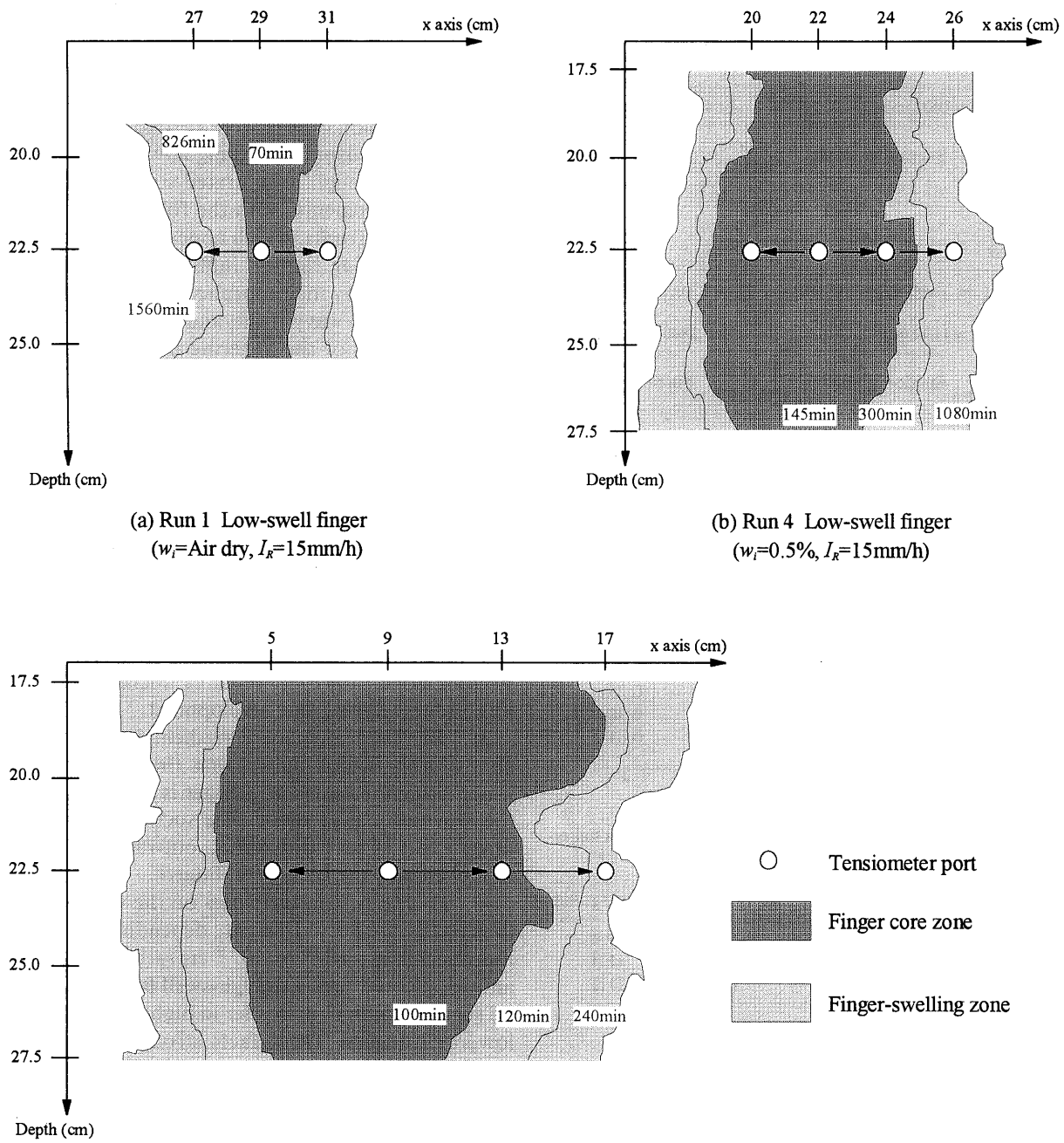

(a) Run 1 Low-swell finger (w_i=Air dry, I_R=15mm/h)

(b) Run 4 Low-swell finger (w_i=0.5%, I_R=15mm/h)

(c) Run 5 High-swell finger (w_i=0.5%, I_R=30mm/h)

Fig. 9. Development of finger-swelling zone with tensiometer ports (The arrows indicate the directions of horizontal suction gradients)

smaller than those of the low-swell fingers in Run 1 (-0.25 and 0.50 at $t=1800$ min) and in Run 4 (0.30 at $t=1800$ min). This may probably indicate that the large value of horizontal suction gradient is not related, in a direct manner, to the velocity of lateral water movement from the center of the finger to the surrounding dry sand. As has already been described, hydraulic conductivities on the wetting process (10^{-8} to 10^{-10} cm/s in the low-swell finger and 10^{-3} to 10^{-4} cm/s in the high-swell finger) dominate the velocity of lateral water movement.

Moisture Profile in Finger-Swelling Zones

We noticed the two successive stages in the suction change taking place inside a swelling zone (Fig. 8). Using the suction changes together with the water characteristic curves in Fig. 6, we can discuss what is happening inside a swelling zone, as follows. In the case of Run 1 (Fig. 8(a)), the sudden decrease of suction takes place along the wetting process ① starting from the air dry condition (stage 1), and the steady state characterized by a constant suction corresponds to the point denoted by a double circle on ① (stage 2). In the cases of Runs 4 and 5 (Fig. 8(b)

Table 7. Horizontal suction gradients in low-swell and high-swell fingers

(a) Run 1 Low-swell finger (w_i=Air dry, I_R=15 mm/h)

x (cm)	t=1002 min		t=1800 min	
	Suction (cmH_2O)	Suction gradient	Suction (cmH_2O)	Suction gradient
27	—	—	23.5	−0.25
29	23.7	0.10	23.0	0.50
31	23.9		24.0	

(b) Run 4 Low-swell finger (w_i=0.5%, I_R=15 mm/h)

x (cm)	t=1100 min		t=1800 min	
	Suction (cmH_2O)	Suction gradient	Suction (cmH_2O)	Suction gradient
20	24.9	0.15	24.8	−0.45
22	25.2	0.60	23.9	0.70
24	26.4	—	25.3	0.30
26	—		25.9	

(c) Run 5 High-swell finger (w_i=0.5%, I_R=30 mm/h)

x (cm)	t=220 min		t=280 min	
	Suction (cmH_2O)	Suction gradient	Suction (cmH_2O)	Suction gradient
5	22.2	−0.25	21.8	−0.25
9	21.2	0.38	20.8	0.38
13	22.7	—	22.3	0.03
17	—		22.4	

Table 8. Estimated (w_{est}) and observed (w_{obs}) water content in finger-swelling zones

Experiment	w_{est} (g/g, %)	w_{obs} (g/g, %)
Run 1 (w_i=Air dry, I_R=15 min/h)	8	9.6
Run 4 (w_i=0.5%, I_R=15 mm/h)	10	11.4
Run 5 (w_i=0.5%, I_R=30 mm/h)	16	11.2

and (c)), the sudden decrease of suction takes place along the wetting process ③ starting from water content of 0.5%, and the steady state also corresponds to the point shown by a double circle on ③. These results indicate that the water condition in a swelling zone always remains at the wetting process, in spite of the fact that the water condition in a core zone of a finger is switched from the wetting to the drying process, as has already been discussed.

Water contents (w_{est}) in these swelling zones can be estimated if the suction changes are used in the water characteristic curves in Fig. 6. In addition actual water contents (w_{obs}) were determined by collecting sand samples in a swelling zone after a test. In Table 8, the estimated water contents are tabulated together with the measured ones. A good agreement between w_{est} and w_{obs} in the swelling zones in Runs 1 and 4 suggests that the water characteristic curve, together with the measured suction values, makes it possible to estimate, with sufficient accuracy, water contents inside a finger. Note, however, that w_{est} in Run 5 is a little larger, than w_{obs}. This discrepancy may occur if water is rapidly redistributed during sampling.

CONCLUSIONS

Two-dimensional tests were carried out to clarify the physical mechanism of fingering flows (non-uniform, unstable flows through unsaturated soils) based on precise suction measurements, with the following conclusions:

1) Wetting fronts, which appear in dry homogeneous sandy soils during rainfall infiltration, can be classified into three types by their morphological characteristics; 1) fingering flow, 2) wavy front, and 3) plane front. Furthermore, two types of the fingering flows can be identified; i.e., low-swell finger and high-swell finger. A big difference between these two types of fingering flow is in their swelling velocities; the high-swell finger swells about ten times higher than the low-swell finger.

2) Each finger, irrespective of its flow type, consists of a central core zone and a marginal swelling zone when it moves downward growing. According to suction measurements, it is found that the water condition in the core zone is switched from the wetting to the drying process. This hysteretic behavior arises from the moisture profile in a finger from tip to tail. The water condition in the swelling zone, however, remains unchanged in the wetting process during the development.

3) The vertical suction gradient in the core zone is almost zero, which means that the downward flow of water along the center of a finger is mainly conducted by the gravitational gradient. The suction gradient inside a finger exists in both horizontal, outward directions in the low-swell and the high-swell fingers.

4) Hydraulic conductivities on the wetting process at finger tails are very different, depending on the type of the finger; i.e., 10^{-8} to 10^{-10} cm/s in low-swell fingers and 10^{-3} to 10^{-4} cm/s in high-swell fingers. The horizontal suction gradient is smaller in high-swell fingers than in low-swell fingers. These facts strongly suggest that the hydraulic conductivity on the wetting process is a primary factor in controlling the swelling due to lateral water movement.

ACKNOWLEDGMENT

The authors would like to express their gratitude to Prof. Nakano of the Faculty of Agriculture, Kobe University, Mr. Imoto of the Graduate School of Agricultural and Life Sciences, the Tokyo University, Prof. Oda of the Department of Civil and Environmental Engineering, Saitama University and Assoc. Prof. Gerrit H. de Rooij of Department of Agricultural Sciences, Saga University for their support and advice in the course of this research.

REFERENCES

1) Annaka, T. and Idesawa, S. (1996): "Physical features of fingering during infiltration into layered glass beads—Growth of fingers due to wetting front instability and the mechanism of finger persistence

(I)—," Trans. Jpn. Soc. Irrig. Drain. Reclam. Engrg., No. 183, pp. 79–88.
2) Baker, R. S. and Hillel, D. (1990): "Laboratory tests of a theory of fingering during infiltration into layered soils," Soil Sci. Soc. Am. J., Vol. 54, pp. 20–30.
3) Bouwer, H. (1966): "Rapid field measurement of air entry value and hydraulic conductivity of soil as significant parameters in flow system analysis," Water Resour. Res., Vol. 2, No. 4, pp. 729–738.
4) Cho, H. (1995): "Three dimensional features of fingering flow: Study on fingering flows in two-layered materials under ponding water (I)," Trans. Jpn. Soc. Irrig. Drain. Reclam. Eng., No. 179, pp. 11–20.
5) de Rooij, G. H. (1995): "A three-region analytical model of solute leaching in a soil with a water-repellent top layer," Water Resour. Res., Vol. 31, pp. 2701–2707.
6) Diment, G. A. and Watson, K. K. (1982): "Stability analysis of water movement in unsaturated porous materials: 3. Experimental studies," Water Resour. Res., Vol. 21, pp. 979–984.
7) Glass, R. J., Steenhuis, T. S. and Parlange, J.-Y. (1989): "Mechanism for finger persistence in homogeneous, unsaturated porous media: Theory and verification," Soil Sci., Vol. 148, pp. 60–70.
8) Glass, R. J., Steenhuis, T. S. and Parlange, J.-Y. (1989): "Wetting front instability, 2. Experimental determination of relationships between system parameters and two-dimensional unstable flow field behavior in initially dry porous media," Water Resour. Res., Vol. 25, No. 6, pp. 1195–1207.
9) Glass, R. J. and Nicholl, M. J. (1996): "Physics of gravity fingering of immiscible fluids within porous media: An overview of current understanding and selected complicating factors," Geoderma, Vol. 70, pp. 133–164.
10) Hill, D. E. and Parlange, J.-Y. (1972): "Wetting front instability in layered soils," Soil Sci. Soc. Am. Proc., Vol. 36, pp. 697–702.
11) Hillel, D. (1993): "Unstable flow: A potential significant mechanism of water and solute transport to groundwater," in: Russo, D. and Dagan, G. (eds.), Water Flow and Solute Transport in Soils, Adv. Series in Agric. Sci., Vol. 20, pp. 123–135.
12) Hillel, D. and Baker, R. S. (1988): "A descriptive theory of fingering during infiltration into layered soils," Soil Sci., Vol. 146, pp. 51–56.
13) Kawamoto, K., Miyazaki, T. and Nakano, M. (1996): "Leaching efficiency depending on the type of fingering flow in sandy soils," Trans. Jpn. Soc. Irrig. Drain. Reclam. Engrg., No. 186, pp. 89–96.
14) Kung, K.-J. S. (1990): "Preferential flow in a sandy vadose zone. 1. Field observation," Geoderma, Vol. 46, pp. 51–58.
15) Liu, Y., Steenhuis, T. S., Parlange, J.-Y. and Selker, J. S. (1991): "Hysteretic finger phenomena in dry and wetted sands," in: Gish, T. J. and Shirmohammadi, A. (eds.), Preferential Flow, Proc. Nat. Sym. on Preferential Flow, 16–17 Dec., Chicago, III. Am. Soc. Agric. Eng., St. Joseph, MI, pp. 160–172.
16) Miyazaki, T. (1993): "Water flow in soils," Marcel Dekker, New York.
17) Philip, J. R. (1975): "Stability analysis of infiltration," Soil Sci. Soc. Am. Proc., Vol. 39, pp. 1042–1049.
18) Raats, P. A. C. (1973): "Unstable wetting fronts in uniform and nonuniform soils," Soil Sci. Soc. Am. Proc., Vol. 37, pp. 681–685.
19) Ritsema, C. J. and Dekker, L. W. (1995): "Distribution flow: A general process in the top layer of water repellent soils," Water Resour. Res., Vol. 31, pp. 1187–1200.
20) Selker, J. S., Steenhuis, T. S. and Parlange, J.-Y. (1992 (a)): "Wetting front instability in homogeneous sandy soils under continuous infiltration," Soil Sci. Soc. Am. J., Vol. 56, pp. 1346–1350.
21) Selker, J. S, Leclerq, P., Parlange, J.-Y. and Steenhuis, T. S. (1992 (b)): "Fingered flow in two dimensions: 1. Measurement of matric potential," Water Resour. Res., Vol. 28, No. 9, pp. 2513–2521.
22) Shiozawa, S. (1983): "Measurement method and accuracy for unsaturated hydraulic conductivity by the steady-state method," Trans. Jpn. Soc. Irrig. Drain. Reclam. Eng., No. 106, pp. 73–79.
23) Steenhuis, T. S., Ristema, C. J. and Dekker, L. W. (1996): "Fingered flow in unsaturated soil: From nature to model, Introduction," Geoderma, Vol. 70, pp. 83–85.
24) Tabuchi, T. (1961): "Infiltration and ensuing percolation in columns of layered glass particles packed in laboratory," Trans. Agric. Eng. Soc. Jpn., No. 1, pp. 27–36.
25) Tamai, N., Asaeda, T. and Jeevaraj, C. G. (1987): "Fingering in two-dimensional, homogeneous, unsaturated porous media," Soil Sci., Vol. 144, No. 2, pp. 107–112.
26) van Genuchten, M. Th. (1980): "A closed-form equation for predicting the hydraulic conductivity of unsaturated soils," Soil Sci. Soc. Am. J., Vol. 44, pp. 892–898.
27) Yao, T.-m. and Hendrickx, J. M. H. (1996): "Stability of wetting fronts in dry homogeneous soils under low infiltration rates," Soil Sci. Soc. Am. J., Vol. 60, pp. 20–28.